THE INFLUENCE OF ANISOTROPIC F REGION ION VELOCITY DISTRIBUTIONS
ON IONOSPHERIC ION OUTFLOWS INTO THE MAGNETOSPHERE

K. Suvanto

Blackett Laboratory, Imperial College, London

M. Lockwood[1]

Rutherford Appleton Laboratory, Chilton, Didcot, England

T. J. Fuller-Rowell

University College, London

Abstract. The contribution to the field-aligned ionospheric ion momentum equation, due to coupling between pressure anisotropy and the inhomogeneous geomagnetic field, is investigated. We term this contribution the "hydrodynamic mirror force" and investigate its dependence on the ion drift and the resulting deformations of the ion velocity distribution function from an isotropic form. It is shown that this extra upforce increases rapidly with ion drift relative to the neutral gas but is not highly dependent on the ion-neutral collision model employed. An example of a burst of flow observed by EISCAT, thought to be the ionospheric signature of a flux transfer event at the magnetopause, is studied in detail and it is shown that the nonthermal plasma which results is subject to a hydrodynamic mirror force which is roughly 10% of the gravitational downforce. In addition, predictions by the coupled University College London – Sheffield University model of the ionosphere and thermosphere show that the hydrodynamic mirror force in the auroral oval is up to 3% of the gravitational force for Kp of about 3, rising to 10% following a sudden increase in cross-cap potential. The spatial distribution of the upforce shows peaks in the cusp region and in the post-midnight auroral oval, similar to that of observed low-energy heavy ion flows from the ionosphere into the magnetosphere. We suggest the hydrodynamic mirror force may modulate these outflows by controlling the supply of heavy ions to regions of ion acceleration and that future simulations of the effects of Joule heating on ion outflows should make allowance for it.

1. Introduction

Recently, Lockwood and Fuller-Rowell [1987a, b] have suggested a causal connection between nonthermal and bi-Maxwellian plasmas in the

---

[1]Also Visiting Honorary Lecturer at Blackett Laboratory, Imperial College, London.

ionospheric F region and sources of the heavy ions which are accelerated to several electron volts at greater altitudes and subsequently flow from the ionosphere into the magnetosphere. In order to look at this suggestion in more detail, this paper assesses the role of temperature anisotropy on plasma dynamics in an inhomogeneous geomagnetic field.

1.1. Observations of Nonthermal and Bi-Maxwellian Plasmas in the Auroral Ionosphere

The presence of non-Maxwellian ion velocity distributions in the auroral ionospheric F region was predicted over a decade ago from considerations of the effects of large ion drifts relative to the neutral gas for various models of the ion-neutral collisional process (see review by St.-Maurice and Schunk [1979]). Some retarding potential analyzer data from the AE-C satellite revealed non-Maxwellian plasma [St.-Maurice et al., 1976], but the spatial/temporal ambiguity problem and the lack of sufficient suitable data meant that the lifetime and occurrence of these distributions remained uncertain. Using the EISCAT incoherent scatter radar, and assuming a bi-Maxwellian ion velocity distribution, Løvhaug and Flå [1986] found very large ion temperature anisotropies ($T_{i\perp}/T_{i\parallel}$ of up to about 2.5) caused by enhanced ion flows during substorms. For these tristatic observations, the ion velocity distribution is sampled along three directions, and each would give a Maxwellian one-dimensional distribution of line-of-sight velocities if the three-dimensional distribution were bi-Maxwellian in form. The effect of a non-Maxwellian line-of-sight ion velocity on the spectra of the scattered signals was predicted theoretically by Raman et al. [1981] and shown to increase rapidly with increasing aspect angle between the look direction and the magnetic field. At large angles to the field (>50°) the spectrum becomes triple humped, having one large central peak with only small shoulders at the ion-acoustic frequency, whereas for small angles (<30°) the spectrum is the normal double-peaked one, characteristic of Maxwellian plasmas. Furthermore, these authors showed that the ion temperature derived from the radar data by assuming a Maxwellian distribution would exceed

the real average (or three-dimensional) one for a non-Maxwellian if the plasma is viewed at a large aspect angle. The old location of the SRI radar at Chatanika (now located at Sondrestromfjord) was ideal for observing such spectra, as the auroral oval (where sufficiently large flows are expected) could be observed at an angle to the field large enough to allow them to become apparent. Indeed, such spectra were observed in the Chatanika data (V. Wickwar, private communication, 1987), but it was impossible to unambiguously attribute them to non-Maxwellian effects as they could be mimicked by velocity changes within the intergration period or by velocity shears within the scattering volume. Definite identification was only recently achieved by Lockwood et al. [1987] by studying the effects of newly-discovered putative ionospheric signatures of flux transfer events at the magnetopause [Todd et al., 1986], observed by EISCAT using the monostatic UK-Polar experiment with a similar auroral viewing geometry to that for the old Chatanika radar site. Recently, Winser et al. [1987b] have used EISCAT Common Programme CP-3-E data to show that the aspect angle dependence of the spectral shape is as predicted by Raman et al. [1981] for the periods when the ion temperature anisotropy, as deduced assuming a bi-Maxwellian form, is larger than expected for the observed ion drift. These observations indicate the presence of non-Maxwellian plasma.

The results of Lockwood et al. [1987; 1988a] showed that the non-Maxwellian plasmas persisted for as long as the ion velocity exceeded the predicted threshold (i.e. longer than ~ 1 minute). Because this is larger than the expected time constants of small-scale processes which would act to destroy the non-Maxwellian velocity distribution (ion-ion collisions, microinstabilities), it is expected that they should exist for large periods of time wherever the relative ion-neutral velocity is sufficiently large. Indeed, Farmer et al. [1988] have reported spectra characteristic of nonthermal plasma observed by the UK-Polar experiment to persist for up to an hour. Lockwood and Fuller-Rowell [1987a, b] have predicted when this should occur, even for steady, moderate convection conditions (and discussed the effects of changes in convection), by making use of the coupled ionosphere-thermosphere UCL model. They have concluded that plasma should be continuously close to the nonthermal threshold in certain regions and suggested a possible connection with large flows of O^+ ions from the ionosphere into the magnetosphere along geomagnetic field lines in these regions.

1.2. Spatial Gradients and Ion-Neutral Coupling Terms in the Kinetic and Momentum Equations

Our aim is to quantify the effect of ion temperature anisotropy and magnetic field inhomogeneity on field-parallel ion flows and assess the implications for modeling and observation of plasma dynamics. In this section we discuss our approximations concerning the kinetic and momentum equations. It is shown that within the approximation scheme to be adopted, the

pressure force can be calculated to lowest order using the ion velocity distribution for a time-independent, spatially homogeneous plasma. In other words, although spatial gradients are of interest in the field-parallel momentum equation it is consistent to neglect them in the kinetic equation in this approximation.

The kinetic equation in the $\overline{E} \times \overline{B}$ drift frame is

$$\Omega \frac{\partial f}{\partial \Theta} = C(f) - \frac{\partial f}{\partial t} - \overline{v} \cdot \frac{\partial f}{\partial \overline{r}}$$

$$- \frac{q}{m} E_\| \frac{\partial f}{\partial v_\|} - g \cdot \frac{\partial f}{\partial \overline{v}} \qquad (1)$$

where f $(\overline{r}, \overline{v}, t)$ is the ion velocity distribution function, Ω the ion gyrofrequency, $E_\|$ the component of the electric field along the geomagnetic field, $\overline{g}$ the gravitational acceleration, and Θ the gyrophase angle in velocity space; the term $C(f)$ accounts for ion-neutral collisions. Coulomb collisions have been neglected because the plasma is only weakly ionized. The corresponding momentum equation describing field-aligned flows may be written as

$$nm \left[\frac{D\overline{u}}{Dt}\right]_\| = - \nu nm (u_\| - u_{n\|}) - \nabla \cdot \overline{\overline{p}} \|$$

$$+ nq E_\| + nmg_\| \qquad (2)$$

where $\overline{u}$ and $\overline{u}_n$ are the ion and neutral drift speeds respectively, $D/Dt = (\partial/\partial t) + \overline{u} \cdot (\partial/\partial \overline{r})$ is the convective derivative, ν is the ion-neutral collision frequency for momentum transfer and the pressure tensor is defined by

$$\overline{\overline{p}} = m \int d^3\overline{v} \, \overline{c} \, \overline{c} \, f \equiv nm \langle \overline{c} \, \overline{c} \rangle \qquad (3)$$

Here $\overline{c}$ is the random part of ion velocity and the angle brackets are defined to denote the ensemble average. In order to derive an expression for the pressure force, the ion velocity distribution has to be known. Some assumptions on the relative magnitudes of the terms in (1) and (2) are needed to enable analytical estimation of the effects caused by anisotropic temperature. The ratios of the last four terms on the right-hand side of (1) to the collisional term can be characterized by the following dimensionless quantitites,

$$\epsilon_1 = 1/\nu T$$

$$\epsilon_2 = V_{th}/\nu L$$

$$\epsilon_3 = qE_\|/\nu m V_{th} \qquad (4)$$

$$\epsilon_4 = g/\nu V_{th}$$

where L and T are the length and time scales associated with spatial and time variations, respectively, and V_{th} is the thermal speed of the ions. We now assume that as far as the form of the distribution function is concerned, ion-neutral collisions dominate over effects associated with spatial gradients, parallel

electric fields and gravitational effects. Also, the typical time scale T for the temporal evolution of f is assumed to be much larger than the relaxation time associated with collisions. In other words, $\varepsilon_1, \varepsilon_2, \varepsilon_3$ and ε_4 must all be $\ll 1$. To lowest order, the distribution function is thus determined by the magnetic field and ion-neutral collisions:

$$\Omega \frac{\partial f}{\partial \theta} = C (f) \qquad (5)$$

In the high-latitude F region $\nu/\Omega \ll 1$, so that f can be written as the sum of a gyrotropic velocity distribution f^0 and a correction δf,

$$f = f^0 + \delta f \qquad (6)$$

where δf is of order ν/Ω, as pointed out by St.-Maurice and Schunk [1979]. In general, the latter term on the righthand side of (6) can be regarded as the correction corresponding to all the neglected terms in (1), f^0 being the gyrotropic distribution for spatially homogeneous and time-independent plasma with rare ion-neutral collisions. It should be noted, however, that neglecting the spatial and time derivatives in (1) is not to say that f should be independent of $\overline{r}$ and t. Merely, we require these derivatives to be small compared with the collisional term.

Although spatial gradients are assumed to be negligible in the kinetic equation, they may be important in the momentum equation (2). This can be seen as follows. The pressure force term in (2) is of the order of nmV_{th}^2/L so that its ratio to the ion-neutral coupling term in the same equation is of order $(V_{th}^2/\nu L \, |u_\parallel - u_{n\parallel}|)$. Our assumption $\varepsilon_2 \ll 1$ implies that $V_{th}^2/\nu L \ll 1$; the above ratio of the pressure and frictional forces can still be comparable to unity because the field-aligned component of the relative ion-neutral drift is much smaller than the ion thermal velocity in our region of interest.

Finally, it should be pointed out that we can put $f = f^0$ in the equation (3) for the pressure tensor. The consistency of this approximation is verified by noting that the pressure force obtained this way is of the order of nmV_{th}^2/L, the correction due to the omitted terms in (1) being approximately $(\nu/\Omega)nmV_{th}^2/L$. The ratio of the correction term to the zeroth-order term is $\ll 1$ as it should be.

Note that the use of a relaxation collision model leads to the result that f^0 is simply the neutral velocity distribution averaged over the gyrophase [Ott and Farley, 1975] so that $u_\parallel = u_{n\parallel}$ in the approximation $f = f^0$. However, this result cannot be used in the frictional term of (2) because this term contains the "large" factor ν (remember our ordering $\varepsilon_i \ll 1$; $i=1,...,4$) and, consequently, the relative field-aligned ion-neutral drift speed must be evaluated to a higher degree of accuracy.

1.3. Ion Outflows From the Ionosphere Into the Magnetosphere

Several recent reviews have discussed the great variety of low-energy ionospheric ion outflows into the magnetosphere which have been observed [Moore, 1984; Lockwood, 1986; Yau and Lockwood,

1988; Horwitz, 1987]. The importance of these flows to magnetospheric plasma composition has been underlined by Chappell et al. [1987] who determined that the typical ion densities in most regions of the magnetosphere can be accounted for by the ionospheric ion outflows alone. The mechanism which injects most ions into the magnetosphere is the "classical" polar wind, a flow of light ions (H^+ and He^+) driven at high and middle latitudes by normal ionospheric plasma density and temperatures via the charge separation, "ambipolar," field-aligned electric field. However, much interest has been focused on low-energy (several eV) heavy ion additions to the polar wind, observed to orginate from the auroral ionosphere, which are more variable than the classical polar wind and hence can act to modulate magnetospheric ion composition. Two distinct sources of such ions have been identified. First, the dayside cleft gives large, continuous fluxes of "upwelling ions" [Lockwood et al., 1985a, b, c; Moore et al., 1986a], which are subsequently dispersed throughout the polar magnetosphere in the "cleft ion fountain" by the convection electric field [Lockwood et al., 1985b; Horwitz and Lockwood, 1985]. Second, low-energy heavy ions are observed in the nightside auroral oval with a variety of pitch angles and energies [e.g., Yau et al., 1985].

In addition to these observations of ionospheric heavy ions in the low-altitude polar magnetosphere, a variety of observations of exceptionally large (i.e., greater than required for the classical polar wind) and warmed ion flows have been made in the auroral ionosphere. Transversely heated O^+ ions have been detected by ion mass spectrometers on satellites [Klumpar, 1979] and rockets [Whalen et al., 1978; Yau et al., 1983; Moore et al., 1986b] and enhanced upward flows of plasma of energy < 1 eV have been reported from topside sounder data [Lockwood and Titheridge, 1981; Lockwood, 1982], from incoherent scatter data [Farmer et al., 1984; Winser et al., 1987a], and from low-altitude satellite mass spectrometers [Lockwood et al., 1985c; Tsunoda et al., 1985; Heelis et al., 1984; Roux et al., 1985]. In all these cases, the authors have suggested these enhanced ionospheric upflows are connected with heavy ionospheric ion flows into the magnetosphere, and in the case discussed by Lockwood et al. [1985c], ions observed in the magnetosphere were traced back to an ionospheric source at the location where the ionospheric upflow was simultaneously observed.

2. Hydrodynamic Mirror Force

In this section, we discuss the pressure force on the ions. As shown in section 1.2, the ion velocity distribution function can be assumed to be gyrotropic; the pressure tensor then takes the form (compare, e.g., with Clemmow and Dougherty [1969, p. 351])

$$P_{ij} = P_\parallel b_i b_j + P_\perp (\delta_{ij} - b_i b_j) \qquad (7)$$

in a Cartesian coordinate system Here $\hat{b}$ is the unit vector parellel with the magnetic field. The pressure force per unit volume is found from (7) by taking the spatial divergence; finally, we

estimate the force of assuming a radial magnetic field, $\overline{B(r)} = B(r) \hat{r}$. The result is

$$- \nabla \cdot \overline{\overline{P}} = \left[- \frac{\partial p_\parallel}{\partial r} + p_\parallel \frac{dB/dr}{B} - p_\perp \frac{dB/dr}{B} \right] \hat{r} \quad (8)$$

The subscripts refer to the directions parallel with and perpendicular to the geomagnetic field respectively. We note in passing that this expression can be given a simple physical interpretation. The first two terms on the right-hand side of equation (8) arise from the fact that a fluid element constrained to move in a flux tube sees a nett force because of variations in (1) pressure and (2) the flux tube cross-sectional area, which is proportional to 1/B (force = pressure x area). The third term is numerically equal to the expectation value of the effective force (per unit volume) associated with magnetic mirroring in single particle dynamics with the guiding-center approximation. From (8) we find that the force per unit volume due to magnetic field inhomogeneity and pressure anisotropy, which will be referred to as the "hydrodynamic mirror force", is given by

$$F_m = nk_B (T_\parallel - T_\perp) \frac{dB/dr}{B} \quad (9)$$

where the parallel and perpendicular temperatures are defined by

$$\tfrac{1}{2} k_B T_\parallel = \tfrac{1}{2} m <c_\parallel^2>$$

$$k_B T_\perp = \tfrac{1}{2} m <c_\perp^2> \quad (10)$$

Note that the force on an ion of a given species, in a given magnetic field, depends only on the perpendicular and parallel temperatures of the species, not the other details of the velocity distribution function.

2.1. Hydrodynamic Mirror Force for a Non-Maxwellian Ion Velocity Distribution

St.-Maurice and Schunk [1979] used a variety of different models for ion-neutral collisions to evaluate the ion velocity distribution function in the case of a supersonic ion flow through the neutral atmosphere; it was found that the kinetic equation with a simple relaxation model for ion-neutral collisions provides a closed-form solution for the distribution function in the limit where spatial and time derivatives can be neglected and ion-neutral collisions are rare, $\nu/\Omega \ll 1$. Also, the plasma is assumed to be linearly stable. This form of the distribution function is characterized by two physical parameters, the Mach number (the ratio of the relative ion-neutral drift velocity and the neutral thermal speed), D', and the neutral temperature T_n. The model exaggerates non-Maxwellian features because of its backscattering nature; it can be used to approximate resonant charge exchange (also an idealization) between O and O^+ and other collisional processes as far as distortions of the field-perpendicular part of the ion velocity distribution function is concerned. A major shortcoming of this model is the fact that no distortions from a Maxwellian shape are predicted in the field-parallel direction. Barakat et al.

[1983] studied the formation of non-Maxwellian velocity distributions using different kinds of collision models in their Monte Carlo simulations. They found that similar departures from a Maxwellian as predicted by the simple relaxation model could be produced by using a more realistic collision model allowing for polarization interactions, provided D' was larger than for the relaxation model. This suggested that the qualitatively good relaxation model could be improved by scaling the parameters D' and T_n. The approach had actually been used by Raman et al. [1981] who replaced D' and T_n by adjustable parameters D* and T* which are to be determined experimentally, as done by St.-Maurice et al. [1976] for satellite retarding potential analyzer data or recently by Moorcroft and Schlegel [1988] for EISCAT data using the spectral synthesis routine by Raman et al. [1981]. The approach has also been justified analytically by Hubert [1984]. We will refer to this semiempirical extension of the theory as the generalized relaxation model. It should be noted that even this generalization does not allow for any distortions from a Maxwellian shape in the field-parallel direction. For the results of Barakat et al. [1983, Table 1] we can estimate that D*/D' > 0.5, because the collision model allowing for both charge exchange and polarization produces more non-Maxwellian features for the electric field strength of 200 mV/m than the pure relaxation model for 100 mV/m. "Non-Maxwellian features" may be quantified by the ratio f_m/f_o, where f_m is the maximum value of the distribution function and f_o the value of the distribution function at $\overline{v} = 0$. From the temperature anisotropies modelled by Barakat et al. [1983], D*/D' ∼ 0.67 for lower field strengths, roughly consistent with the observations of Moorcroft and Schlegel [1988].

However, the assumption of a linearly stable plasma does not hold for very large drifts. The distribution function discussed above has been predicted to become unstable to the Post-Rosenbluth [Ott and Farley, 1975; St.-Maurice and Schunk, 1978] and ion cyclotron microinstability [Lakhina and Bhatia, 1984; Suvanto, 1988a] if D* is larger than about 1.3. The distribution function itself will be modified by interactions between the particles and the large-amplitude waves associated with the instability [Suvanto, 1988b]. St.-Maurice [1978] has argued that the plasma will become only marginally unstable because of the wave-induced diffusion in velocity space. This may explain the behavior of D*/D' as a function of D' (see section 2.3).

The generalized relaxation model, as employed by Raman et al. [1981], gives

$$T_\parallel = T^*$$

$$T_\perp = T^* (1 + D^{*2}) \quad (11)$$

$$T_i = T^* (1 + \tfrac{2}{3} D^{*2})$$

where T_i is the average (or three-dimensional) ion temperature. Using arguments similar to those presented in section 1.2, one can show that the ion-neutral coupling term can be regarded as the dominant one in the ion energy equation, which then takes the familiar form
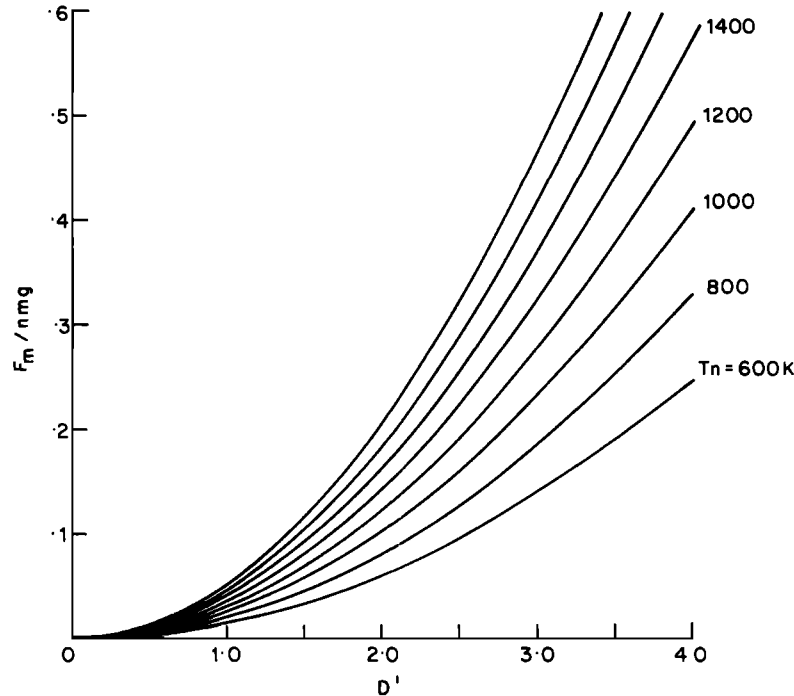
Fig. 1. The hydrodynamic mirror force for the pure relaxation model, as a fraction of gravity and as a function of the Mach number D'.

$$T_i = T_n \left(1 + \frac{2}{3} D'^2\right) \qquad (12)$$

Here T_n is the nautral temperature. The hydrodynamic mirror force associated with a non-Maxwellian distribution is found from (9), (11), and (12) to be

$$F_m = nk_B T_n \left[\frac{1 + \frac{2}{3} D'^2}{1 + \frac{2}{3} D*^2}\right] D*^2 \frac{3}{r} \qquad (13)$$

where B has been assumed to be proportional to r^{-3}.

2.2. Hydrodynamic Mirror Force as a Function of Drift

We now can investigate the magnitude of the hydrodynamic mirror force as a function of the relative ion-neutral drift speed. Figure 1 assumes the pure relaxation model ($D*/D' = 1$) for D' between 0 and 4 (see section 2.4 for predictions of D' values) and F_m is shown for different values of the neutral temperature, and as a fraction of the gravitational downforce (nmg). For the typical neutral temperature $T_n=1000$ K the extra upforce is more than 10% of gravity if D'>2. Figure 2 shows (F_m/nmg) as a function of D*/D' (roughly speaking, as a function of the collision model) for five fixed values of D'. Clearly, F_m maximizes at D*/D = 1, corresponding to the pure relaxation model. It is interesting to consider whether deviations from this collision model affect the value of F_m seriously. For D'=1, the magnitude of F_m at D*/D'=0.5 is only 40% of the maximum value but for

D'=4 the corresponding figure is as much as 80%. We conclude that especially for large drifts, the value of the hydrodynamic mirror force is not very sensitive to the collision model used. It should be noted that, this is true only for the generalized relaxation model, which may over-estimate the temperature anisotropy and thus the magnitude of the hydrodynamic mirror force.

2.3. Hydrodynamic Mirror Force in a Flow Burst Event

There is very little data available concerning the possible values of D*/D' in the real ionosphere. Figure 3a, which is based on fits from RPA data [St.-Maurice and Schunk, 1979] and fits to EISCAT spectra, during the flow burst event described by Todd et al. [1986], shows the estimated dependance of D*/D' on D'. The values of D' can be evaluated from the EISCAT data because of two important features of the flow burst events. The first is that for this event the ion flow is largely aligned with the radar line-of-sight (see discussion given by Lockwood et al. [1988a] on this event) and the second is that the duration of the burst of enhanced flow is short compared with the response times of the neutral winds, composition and temperature. Consequently, the ion and neutral velocities within the flow burst are known from the ion velocities observed within and around the burst, respectively (the latter being almost zero). Hence the relative ion-neutral drift, V_d, can be computed. In addition, the intercepts of regression fits of observed ion temperature (derived assuming a Maxwellian plasma) as a function of the square of the observed ion velocity, yield the neutral temperature for each scattering volume [see Lockwood et al., 1987].
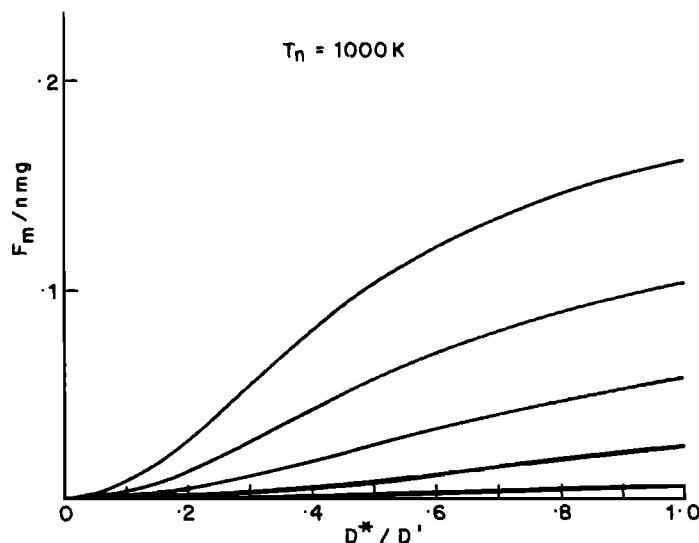
Fig. 2. The hydrodynamic mirror force as a function of the ratio D^*/D' associated with deviations from the relaxation collision model.

Hence the only unknown in D' is the neutral mass which is assumed to be 16 amu (O^+). The uncertainties in D' are estimated from the experimental error in ion velocity and the error in T_n (computed from the regression fits at the 2σ level). The values of D^* are computed by fits of the Raman et al. spectra to the observed spectra (both shown in Figure 2 of Lockwood et al. [1988a] and should be regarded as having an error of roughly 0.1. For small drifts, D^*/D' is almost constant and close to 1; at $D' \sim 1.3$ the ratio falls off to about 0.7 but remains larger than 0.5 for $D' < 2.5$. It is interesting to note that these data appear to show the value of D^* increasing to
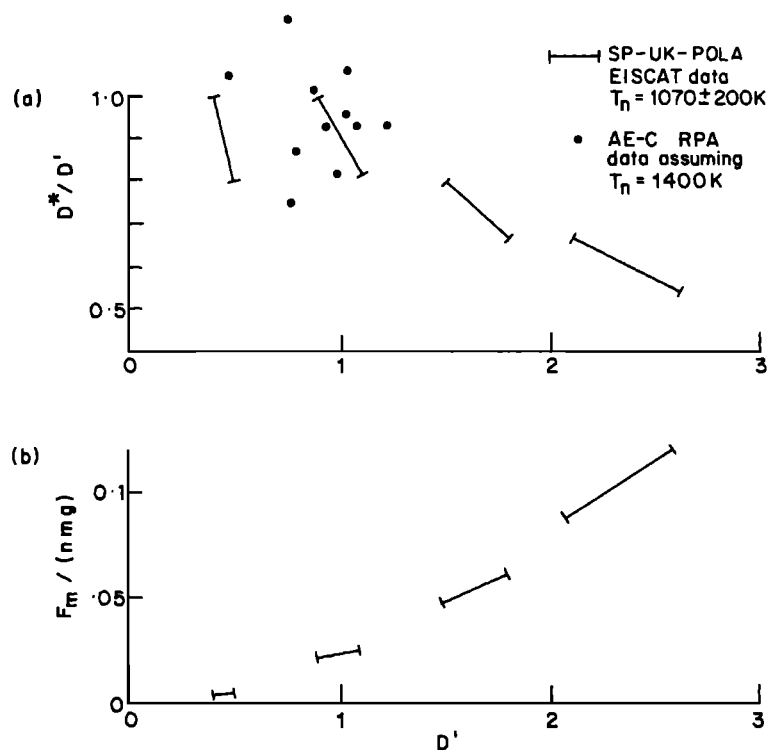

Fig. 3. (a) fits to the EISCAT data presented by Lockwood et al. [1987a,b], as a function of D' (see text). Also shown are values from the RPA data presented by St.-Maurice et al. [1976]. (b) The hydrodynamic mirror force as a function of D' for the D^*/D' values given in Figure 3a. The error bars reflect the uncertainty in D' alone.

close to the limit ($D* \sim 1.3$) where the ion
velocity distribution is predicted to become
unstable to the ion cyclotron and Post-Rosenbluth
instabilities due to the temperature anisotropy
and the positive slope of the perpendicular
distribution. These EISCAT data are thought to
show the ionospheric signature of a flux transfer
event (FTE) [Todd et al., 1986] and the plasma was
shown to be driven into a non-Maxwellian by
Lockwood et al. [1987, 1988a]. The variation of
the hydrodynamic mirror force with $D*/D'$, taken
from figure 3a, is shown in Figure 3b. The
magnitude of the force exceeds 10% of gravity for
$D'=2.5$, observed at the centre of the FTE. This
value of D' is somewhat larger than the predicted
in the centre of an ionospheric signature of an
FTE by Lockwood et al. [1988b], however, it is
comparable with that predicted by these authors
for the region of close field lines on either
flank of the FTE.

Lockwood et al. [1988b] point out that both the
hydrodynamic mirror force calculated here and the
effect of a rise in the field-parallel ion
temperature due to the transient burst of Joule
heating which accompanies the FTE (as predicted
for a homogeneous geomagnetic field by Gombosi and
Killeen [1987]) should drive upward flows of ions
and any such ions which are subject to further
acceleration (to ~ 100 eV energies) can reach the
dayside magnetopause and should be present on the
open flux tubes of the centre of the FTE and on
closed flux tubes in the wake of the FTE. They do
indeed find such ions in examples observed by the
AMPTE UKS satellite where the FTE is thought to
have been on the magnetopause and driving
ionospheric ion flows for longer than the transit
time of the ions from the ionosphere to the
magnetopause. If the source of these ions is
indeed the ionospheric FTE signature, the relative
contribution of hydrodynamic force and transient
Joule heating is not yet known.

2.4. Global Predictions of Hydrodynamic Mirror Force

Lockwood and Fuller-Rowell [1987a; b] have
presented predictions of the spatial distribution
of D' and T_n from the three-dimensional, time-
dependent, UCL-Sheffield University global model
of the coupled ionosphere-thermosphere system
[Fuller-Rowell et al., 1987]. In this paper we
make use of these predictions to evaluate the
hydrodynamic mirror force. The model self-
consistently evaluates the plasma densities and
temperatures and the neutral wind, temperature and
composition for assumed patterns of the convection
electric field and auroral particle precipitation.
For a given location, UT, magnetic activity and
time of year, all the parameters in D' can be
evaluated for the patterns adopted. The results
presented by Lockwood and Fuller-Rowell were for
December solstice and a solar F10.7 flux index of
165 (near sunspot maximum) and for a negative B_y
component of the interplanetary magnetic field,
simulated by using the Heppner and Maynard [1983]
A-2 model of convection equipotentials in the
northern hemisphere and the B-2 model in the
southern hemisphere (reproduced in Figure 7 of
Rees et al. [1985]). Figure 1 of Lockwood and
Fuller-Rowell [1987b] shows results for D' for two
sets of conditions. First, moderately quiet

conditions ($K_p \sim 3$), were simulated by using a
TIROS auroral activity level of 7 [Fuller-Rowell
and Evans, 1987] with a cross-cap potential of 76
kV and allowing the model to attain steady state
in a diurnal sense. The other set of conditions
was for immediately followwing a southward turning
of the interplanetary magnetic field, in that the
cross-cap potential is increased to 152 kV, the
model having achieved steady state immediately
prior to the increase for the quiet conditions (76
kV, TIROS level 7). In the case with this
transient increase of cross-cap potential, it is
assumed the thermospheric winds and composition
have not had sufficient time to respond, nor has
the polar cap radius in accordance with Faraday's
law (as described by Siscoe and Huang [1983] and
Lockwood et al. [1986a]). Increases in cross cap
potential and subsequent expansion of the polar
cap have recently been reported by Lockwood et al.
[1986a,b], and the response of the convection ion
flow speeds to IMF B_z variations have been
discussed by Rishbeth et al. [1985] and Etemadi et
al. [1988].

In this section it is assumed that $D*$ is
roughly equal to D'. Table 1 of Lockwood and
Fuller-Rowell [1987b] shows that for O^+ ions at
300 km, D' is everywhere less than about 0.9 for
the quiet conditions, this maximum value rising to
near 1.8 following the transient increase in
cross-cap potential. Figure 3a indicates that $D*$
should be roughly equal to D' for the range of D'
predicted for the quiet condition (0 D' 0.9)
but the use of $D* = D'$ may not be valid for the
peak D' predicted after the transient convection
enhancement. However, Figure 3a indicated that
for D' of 1.8, $D*/D'$ is roughly 0.7, and Figure 2
shows that the hydrodynamic mirror force at $D*/D'$
$= 0.7$ is more than 90% of its value for $D*/D = 1.0$. Hence we estimate that the adoption of $D*/D'$
$= 1$ will not cause an over-estimation of the
upforce of more than 10%.

Figure 4 shows the hydrodynamic mirror force
predicted by the UCL-Sheffield model, using (13)
with $D* = D'$. The values for O^+ ions at a
constant pressure level which is everywhere very
close to an altitude of 300 km, and the upforce is
shown as a ratio of the gravitational downforce on
the ions to give some estimation of the importance
of the upforce due to the inhomogeneous magnetic
field in the ion momentum equation. Each contour
plot is in a geographic latitude – solar local
time frame and is a snapshot for 18 UT and
corresponds to the D' plots given in Figure 1 of
Lockwood and Fuller-Rowell [1987b]. Figures 4a
and 4b show the predictions for the quiet, steady
state conditions for the north and south (winter
and summer) polar regions respectively. Figures
4c and 4e show the equivalent plots for
immediately after the transient convection
enhancement. For the quiet conditions, the
additional upforce is everywhere less than 2.7% of
the gravitational downforce in winter and less
that 1.7% in summmer. Without modelling of the
plasma dynamics along the flux tube, which is
beyond the scope of this paper, it is not clear if
this is a significant factor in terms of driving
ion upflows. The peak upforce is found in the
dayside auroral throat region, where the large
westward neutral winds established in the
afternoon auroral oval by ion drag meet the
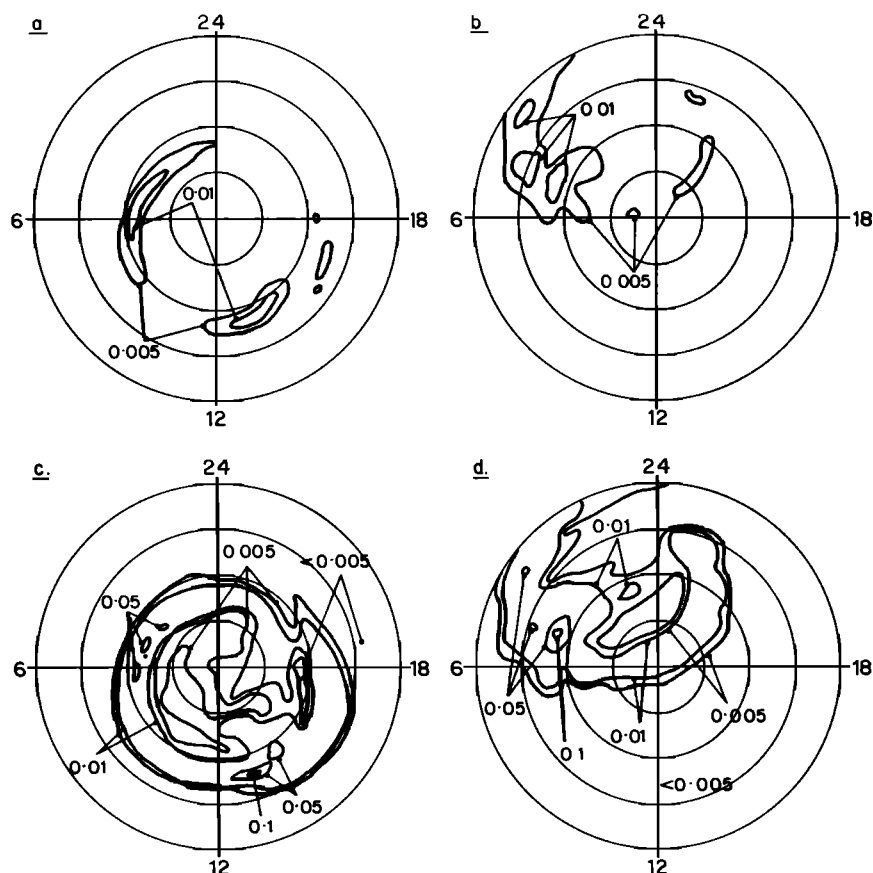eastward convecting plasma of the morning sector;

Fig. 4.   Predicted values of the hydrodynamic mirror force on O^+ ions at 300 km for 1800 UT and December solstice with F10.7 = 165 and B_y 0.   Contours of F_m/nmg are shown as a function of solar local time (SLT) and geographic latitude over the range 50°-90°;   4a and 4c are for the northern (winter) hemisphere and 4b and 4d are for the southern (summer) hemisphere.   For 4a and 4b the cross-cap potential is 76 kV and the ionosphere-thermosphere system has achieved steady state;   4c and 4d show the upforce immediately after an increase from 76 to 152 kV under the same conditions.

as such flows are almost completely oppositely directed, the ion drift relative to the neutral gas is roughly the arithmetic sum of the neutral and ion speeds. Note that at this UT the throat is after 1200 SLT for the northern hemisphere and before 1200 SLT in the southern, but in an MLT-invariant latitude frame it is in the pre-noon sector in both cases (see convection patterns given in Figure 7 of Rees et al. [1985]). The second, smaller peaks of the upforce are found in the dawn cell auroral oval. These are not as marked as the corresponding peaks in D', because T_n is not as large as in the cusp region (see Figure 1c of Lockwood and Fuller-Rowell [1987a]). However, the higher T_n in the summer hemisphere causes the upforce to be 1.5% of gravity in the dawn oval, compared with only 1% in winter. The origin of the dawn-dusk asymmetry in D' in the auroral oval has been discussed by Lockwood and Fuller-Rowell [1987a, and references therein].

Whether or not these upforces are significant in terms of ion dynamics, comparison of Figures 4c and 4e with Figures 4a and 4b shows that dramatic increases are caused by the transient increase in convection. For these cases the upforce rises to

10% of gravity in both hemispheres in the cusp. The upforce in the dawn auroral oval is not enhanced to the same extent.

3.   Discussion and Conclusions

We have studied the effect of an anisotropic ion velocity distribution on field-aligned ion flows in the high latitude ionosphere. Such distribution functions produce an additional upward force on F region plasma (between about 200 and about 500 km altitude) that is usually neglected in numerical simulations of ion dynamics and densities. It is found that the value of D*/D' does not greatly affect this upforce. The magnitude of the hydrodynamic mirror force increases rapidly with the Mach number D'.

We have investigated the magnitude of the upforce within a flow burst event, observed by the EISCAT radar and shown by Todd et al. [1986] to be fully consistent with the expected ionospheric signature of a flux transfer event. It is found that in the center of this event the ion drift is sufficiently large for the hydrodynamic mirror force to become as large as 10% of the

gravitational downforce on O^+ ions at 450 km altitude. Such a large factor would appear to be too large to ignore in the study of ion dynamics and we recommend future simulations should allow for such effects. The increased upforce is applied transiently in this case (for less than about 5 min).

In addition, we have made use of the UCL-Sheffield University coupled model of the ionosphere-thermosphere system to study this effect under more stable conditions. For moderate geomagnetic activity (Kp ~ 3) we find that the peak upforce is only about 3% of gravity in the cusp region in winter and 2% in summer. However, if the cross-cap potential then suddenly rises from 76 to 152 kV (due to a strong southward turning of the IMF) these values rise to near 10%, similar to the value deduced for the FTE signature event. In this case the large upforce could be present in the cusp for a period of up to several hours while the neutral wind and plasma convection patterns respond to the change, and the upforce ratio would gradually decline to a value not much greater than the 2-3% prior to the convection enhancement. Note, however, that this upforce is still a short-lived transient as far as an individal convecting flux tubes is concerned, being applied for the duration of its transit across the "hot spot" of high D' predicted by Lockwood and Fuller-Rowell [1987b], which is typically 5-10 min.

A secondary, much smaller peak in the hydrodynamic mirror force (1-1.5% of gravity) is found in the dawn auroral oval, and this is not so dramatically increased by convection enhancements. However, in this case the flux tubes will convect along the auroral oval and hence remain within the region of enhanced upforce. In this case, the principal effect could be an adjustment of the ambipolar field and an increase in the O^+ scale height. As discussed by Moore [1980; 1984] and Lockwood [1984] this can still be a major factor in ion dynamics by increasing the densities of O^+ ions at higher altitudes where the probability of charge exchange with geocoronal hydrogen atoms is reduced and where acceleration mechanisms can drive heavy ion outflows.

3.1. Comparisons With Available Observations

The results presented in Figure 4 are for one set of season/sunspot cycle conditions and a single UT and in a geographic frame of reference. In order fully to contrast with statistical surveys of satellite data on ion flows, averaging of large seasonal and sunspot number bins, and over all UT should be carried out and the results given in an MLT-invariant latitude frame. However, we can still draw certain parallels, without employing the massive computation time for so many runs of the coupled UCL-Sheffield University model, by noting that the maximum upforce (and Joule heating) is predicted in the convection throat region (before magnetic noon) with a smaller peak in the post-midnight auroral oval. A great many of the statistical surveys of ionospheric heavy ion upflows show similar features. The survey of DE 1-RIMS data on 0-60 eV (relative to spacecraft potential) O^+ ions by Lockwood et al. [1985a] shows the pre-noon throat region to be a regular and strong source of O^+

ions in "upwelling ion events." Moore et al. [1986a] have studied one such event in detail and found the ionosperic source to lie within a rapid convection "jet," implying that ion-neutral frictional heating and distortions of the ion velocity distribution function may indeed be a factor, as suggested by Lockwood and Fuller-Rowell [1987a]. The comparison of simultaneous data from the DE 1 and 2 satellites by Lockwood et al. [1985c] shows upwelling ion events originate in upflows of very low energy plasma in the cusp ionosphere.

Craven et al. [1985] have deduced that this region is also the source of moleculer ions observed in the polar magnetosphere. We note that this calls for an upforce on the molecular ions at very low altitudes, and the hydrodynamic mirror force and collisions with neutral molecules in the presence of strong ion drifts (i.e., where D' is large) would be a strong candidate for such an upforce.

Studies of nightside auroral ionospheric ion upflows are much more complex, due to the variety of energy ranges, pitch angle distributions and energising altitudes of the ions. Nevertheless, there is a persistent dawn-dusk asymmetry in the surveys of these flows, similar to that predicted in Figure 4 for the hydrodynamic mirror force. Yau et al. [1985] have evaluated the average upflux of O^+ ions observed by EICS instrument on DE 1 in the energy range 0.01-1 keV (relative to spacecraft potential). Their study contained data for Kp = 3-5 and from two periods which together cover the entire falling phase of the last solar cycle. For both periods the morphology of O^+ flow is the same (see their Figure 4) with peak average flows in the auroral oval which exceed 5 x 10^8 cm^2 s^{-1} for the 1500-2100 MLT quadrant (all fluxes being normalized to 1000 km altitude). This dawn-dusk asymmetry about local midnight is also reported in the occurence frequency of a variety of upflowing low-energy ionospheric ion events: of thermal ions in the topside ionosphere inferred from topside soundings [Lockwood, 1983]; of "transversely accelerated ion" events at energies >5 eV observed by the ISIS 2 satellite at 1400 km [Klumpar, 1979] and of upgoing uni-directional O^+ flows (energy > 10 eV) observed by DE 1-EICS [Sagawa et al., 1987]. The dawn-dusk asymmetry in these data has usually been ascribed to a variation in the acceleration mechanism with MLT, usually thought to be associated with the known pattern of field-aligned currents which are one possible cause of the acceleration. However, a secondary factor is suggested by Figure 4, in that these observed asymmetries in ion outflows could be associated with an MLT variation in the strength of the source of O^+ ions which feeds ions into the acceleration region.

Considerable upfluxes of ions along the geomagnetic field lines have been reported from EISCAT data by Farmer et al. [1984] and Winser et al. [1987a] following increases in Joule heating and rises in ion temperature. These data are from the tristatic EISCAT system; however, the unfavorable viewing geometry and differences in system noise at the three receiving sites makes it difficult to quantify the ion temperature anisotropy in these events. For the event reported by Winser et al. [1988] and Jones et al. [1988], the observing geometry is ideal and the

Joule heating is caused by a reversal of the ion convection from westward to eastward (near the Harang discontinuity) to which the neutral winds cannot respond. The upflows observed by Farmer et al. [1984] follow a westward convection enhancement due to a geomagnetic substorm. In a similar event, Løvhaug and Flå [1986] were able to employ the tristatic configuration of EISCAT to determine that a large ion temperature anisotropy did indeed result from the enhanced ion convection. The observations of upflows by Winser et al. [1987a] and Farmer et al. [1984] correspond to the regions of moderate upforce predicted here for the post-midnight sector under steady state conditions and the afternoon sector following a convection enhancement, and hence do suggest that heating and distribution function changes due to ion-neutral collisions may indeed be important in driving upflows of ionospheric plasma.

3.2. Relevance to Models of Ion Upflows

In this section, we discuss some situations in data analysis and numerical simulations where the assumption of isotropic plasma can lead to erroneous results. Consider first the modeling of field-aligned velocity profiles observed by incoherent scatter radar. If the ion temperature anisotropy is neglected (by regarding the field-aligned temperature measured in the experiment as the average one), the last two terms in (8) cancel and the deduced upward pressure force on the ions will be too small by the amount of the hydrodynamic mirror force. On the other hand, regarding the field-parallel ion temperature as equal to a value of the field-perpendicular temperature measured, e.g., by a retarding potential analyzer of a low-altitude polar-orbiting satellite, is likely to yield an over estimate of the upward pressure force because typically $T_\parallel < T_\perp$. Finally, it should be pointed out that the ion energy equation (12) used in numerical modeling yields the average ion temperature T_i. Assuming isotropy and, in particular, that $T_\parallel = T_\perp$, will again lead to an erroneous value for the field-aligned upforce (probably to an overestimate because we expect $T_\parallel < T_\perp$). We note that Schunk et al. [1975] allowed for anisotropy effects in their study of the plasma density profiles for assumed zero flow at a boundary in the topside ionosphere but did not consider the effects on plasma flows out of the ionosphere.

Large upflows in assoication with frictional and Joule heating have been reported by Winser et al. [1988]. To quantify the contribution of the hydrodynamic mirror force to the transient expansion modelled by Gombosi and Killeen [1987] is a nontrivial problem. Let us consider the initial expansion before the plasma density profile (and hence the ambipolar field) has responded to the heating. By balancing the hydrodynamic mirror force with the ion-neutral drag force we find that the ion flow relative to the neutral gas will be limited to a few metres per second or less. At greater altitudes, the collision frequency becomes smaller and larger velocities are possible; however, at some point the approximation scheme discussed in section 1.2 breaks down because the ion velocity distribution

is then determined by other effects than ion-neutral collisions.

References

Barakat, A. R., R. W. Schunk, and J.-P. St.-Maurice, Monte Carlo calculations of the O^+ velocity distribution in the auroral ionosphere, J. Geophys. Res., 88, 3237-3241, 1983.

Chappell, C. R., T. E. Moore, and J. H. Waite, Jr., The ionosphere as a fully adequate source of plasma for the Earth's magnetosphere, J. Geophys. Res., 92, 5896-5910, 1987.

Clemmow, P. C. and J. P. Dougherty, Electrodynamics of Particles and Plasmas, Addison-Wesley, Reading, Mass., 1969.

Craven, P. D., R. C. Olsen, C. R. Chappell, and L. Kakani, Observations of molecular ions in the Earth's magnetosphere, J. Geophys. Res., 90, 7599, 1985.

Etemadi, A., S. W. H. Cowley, M. Lockwood, B. J. I. Bromage, D. M. Willis, and H. Luhr, The dependence of high latitude dayside ionospheric flows on the north-south component of the IMF: A high time resolution correlation analysis using EISCAT "Polar" and AMPTE UKS and IRM data, Planet. Space Sci., 36, 471-487, 1988.

Farmer, A. D., M. Lockwood, R. B. Horne, B. J. I. Bromage, and K. S. C. Freeman, Field-perpendicular and field-aligned plasma flows observed by EISCAT during a prolonged period of northward IMF, J. Atmos. Terr. Phys., 46, 473-488, 1984.

Farmer, A. D., M. Lockwood, T. J. Fuller-Rowell, and U. P. Løvhaug, Model predictions of the occurrence of non-Maxwellian plasma, and analysis of their effects on EISCAT data, J. Atmos. Terr. Phys., 50, 487-499, 1988.

Fuller-Rowell, T. J., and D. S. Evans, Height-intergrated Pedersen and Hall conductivity patterns inferred from the TIROS/NOAA satellite data, J. Geophys. Res., 92, 7606-7618, 1987.

Fuller-Rowell, T. J., D. Rees, S. Quegan, G. J. Bailey, and R. J. Moffett, Interactions between neutral thermospheric composition and the polar ionosphere using a coupled ionosphere-thermosphere model, J. Geophys. Res., 92, 7744-7748, 1987.

Gombosi, T. I., and T. L. Killeen, Effects of thermospheric motion on the polar wind; A time-dependent numerical study, J. Geophys. Res., 92, 4725-4729, 1987.

Heelis, R. A., J. D. Winningham, M. Siguira, and N. C. Maynard, Particle acceleration parallel

and perpendicular to the magnetic field observed by DE 2, J. Geophys. Res., 89, 3893, 1984.

Heppner, J. P. and N. C. Maynard, High latitude electric field models, paper presented at Chapman Conference on Magnetospheric Currents, AGU, Irving, VA., April 5-8, 1983.

Horwitz, J. L., Core plasma in the magnetosphere, Rev. Geophys., 25, 579-587, 1987.

Horwitz, J. L., and M. Lockwood, The cleft ion fountain: A two-dimensional kinetic model, J. Geophys. Res., 90, 9749-9762, 1985.

Hubert, D., Non-Maxwellian velocity distribution functions and incoherent scattering of radar waves from the auroral ionosphere, J. Atmos. Terr. Phys., 46, 601-612, 1984.

Jones, G. O. L., P. J. S. Williams, K. J. Winser, M. Lockwood and K. Suvanto, Large plasma velocities along the magnetic field lien in the auroral zone, Nature, 336, 231-232, 1988.

Klumpar, D. M. Transversely accelerated ions: An ionospheric source of hot magnetospheric ions, J. Geophys. Res., 84, 4229,1979.

Lakhina, G. S. and K. G. Bhatia, Ion cyclotron instability in the auroral F-regions, J. Geophys. Res., 89, 9845-9849, 1984.

Lockwood, M., Thermal ion flows in the topside auroral ionosphere and the effects of low-altitude, transverse acceleration, Planet. Space Sci., 30, 595-609, 1982.

Lockwood, M., Thermospheric control of the auroral source of O$^+$ ions for the magnetosphere, J. Geophys. Res., 89, 301-315, 1984.

Lockwood, M., Low-Energy ion flows into the magnetosphere, Adv. Space Res., 6 (3), 63-77, 1986.

Lockwood, M., and T. J. Fuller-Rowell, The modelled occurrrence of nonthermal plasma in the ionospheric F region and the possible consequences for ion outflows into the magnetosphere, Geophys. Res. Lett., 14, 371-374, 1987a.

Lockwood, M., and T. J. Fuller-Rowell, Correction to "The modelling occurrence of nonthermal plasma in the ionospheric F region and possible consequences for ion outflows into the magnetosphere," Geophys. Res. Lett., 14, 581-582, 1987b.

Lockwood, M., and J. E. Titheridge, Ionospheric origin of magnetospheric O$^+$ ions, Geophys. Res. Lett., 8, 381-384, 1981.

Lockwood, M., J. H. Waite, Jr., T. E. Moore, J. F. E. Johnson, and C. R. Chappell, A new source of suprathermal O$^+$ ions near the dayside polar cap boundary, J. Geophys. Res., 90, 4099-4116, 1985a.

Lockwood, M., M. O. Chandler, J. L. Horwitz, J. H. Waite, Jr., T. E. Moore, and C. R. Chappell, The cleft ion fountain, J. Geophys. Res., 10, 9736-9748, 1985b.

Lockwood, M., T. E. Moore, J. H. Waite, Jr., C. R. Chappell, J. L. Horwitz, and R. A. Heelis, The geomagnetic mass spectrometer-Mass and energy dispersions of ionopheric ion flows into the magnetosphere, Nature, 316, 612-613, 1985c.

Lockwood, M., A. P. van Eyken, B. J. I. Bromage, D. M. Willis, and S. W. H. Cowley, Eastward propagation of a plasma convection enhancement following a southward turning of the interplanetary magnetic field, Geophys. Res. Lett., 13, 72-75, 1986a.

Lockwood, M., A. P. van Eyken, B. J. I. Bromage, J. H. Waite, Jr., T. E. Moore, and J. R. Doupnik, Low-energy outflows from the ionosphere during a major polar cap expansion-Evidence for equatorward motion of inverted-V structures, Adv. Space Res., 6(3), 93-101, 1986b.

Lockwood, M., B. J. I. Bromage, R. B. Horne, J.-P. St.-Maurice, D. M. Willis, and S. W. H. Cowley, Non-Maxwellian ion velocity distributions observed using EISCAT, Geophys. Res. Lett., 14, 111-114, 1987.

Lockwood, M., K. Suvanto, J.-P. St.-Maurice, K. Kikuchi, B. J. I. Bromage, D. M. Willis, S. R. Crothers, H. Todd, and S. W. H. Cowley, Scattered power from non-thermal F-region plasma observed by EISCAT-Evidence for coherent echoes?, J. Atmos. Terr. Phys., 50, 467-486, 1988a.

Lockwood, M., M. F. Smith, and G. L. Siscoe, Ionospheric ion upwelling in the wake of flux transfer events at the dayside magnetopause, J. Geophys. Res., 93, 5641-5654, 1988b.

Løvhaug, U. P., and T. Flå, Ion temperature anisotropy in the auroral F region as measured with EISCAT, J. Atmos. Terr. Phys., 48, 959-971, 1986.

Moorcroft, D. R., and K. Schlegel, Evidence for non-Maxwellian velocity distributions in the F-region, J. Atoms. Terr. Phys., 50, 455, 1988.

Moore, T. E., Modulation of terrestrial escape flux composition (by low-altitude acceleration and charge exchange chemistry), J. Geophys. Res., 85, 2011-2116,1980.

Moore, T. E., Superthermal ionospheric outflows, Rev. Geophys. Space Phys., 22, 264-274, 1984.

Moore, T. E., M. Lockwood, M. O. Chandler, J. H. Waite, Jr., C. R. Chappell, A. Persoon, and M. Suguira, Upwelling O$^+$ ion source characteristics, J. Geophys. Res., 19, 7019-7031, 1986a.

Moore, T. E., C. J. Pollock, R. L. Arnold, and P. M. Kintner, Preferential O$^+$ heating in the topside ionsphere, Geophys. Res. Lett., 13, 901-904, 1986b.

Ott, E. and D. T. Farley, Microinstabilities and the production of short-wavelength irregularities in the auroral F region, J. Geophys. Res., 80, 4599-4602, 1975.

Raman, R. S. V., J.-P. St.-Maurice, and R. S. B. Ong, Incoherent scattering of radar waves in the auroral ionosphere, J. Geophys. Res., 86, 4751-4762, 1981.

Rees, D., R. Gordon, T. J. Fuller-Rowell, M. F. Smith, G. R. Carignan, T. L. Killeen, P. B. Hays, and N. W. Spencer, The composition, structure, temperature and dynamics of the upper thermosphere in the polar regions during October to December 1981, Planet. Space Sci., 33, 627-666, 1985.

Rishbeth, H., P. R. Smith, S. W. H. Cowley, D. M. Willis, A. P. van Eyken, B. J. I. Bromage, and S. R. Crothers, Ionospheric response to changes in the interplanetary magnetic field observed by EISCAT and AMPTE-UKS, Nature, 318, 415-416, 1985.

Roux, D., J. J. Berthelier, V. A. Gladyshev, L. V. Zinin, V. D. Maslov, and M. L. Pivovarov, Vertical transport of O$^+$ ions at high latitudes, in Results of the ARCAD-3 Project and of the Recent Programmes in Magnetospheric

and Ionospheric Physics, p.381, France
Cepadues, Toulouse, 1985.

Sagawa, E., A. W. Yau, B. A. Whalen, and W. K.
Peterson, Pitch angle distributions of low-
energy ions in the near-Earth magnetosphere, J.
Geophys. Res., 92, 12,241-12,254, 1987.

Schunk, R. W., W. J. Raitt, and P. M. Banks,
Effect of electric fields on the daytime high-
latitude E and F regions, J. Geophys. Res., 80,
3121-3130, 1975.

Siscoe, G. L., and T. S. Huang, Polar cap
inflation and deflation, J. Geophys. Res., 90,
543-547, 1983.

St.-Maurice, J.-P., On a mechanism for the
formation of VLF electrostatic emissions in the
high latitude F region, Planet. Space Sci., 26,
801-816, 1978.

St.-Maurice, J.-P., W. B. Hanson and J. C. G.
Walker, Retarding Potential Analyzer
Measurement of the effect of ion-neutral
collisons on the ion velocity distribution in
the auroral ionosphere, J. Geophys. Res., 81,
5438-5446, 1976.

St.-Maurice, J.-P. and R. W. Schunk, Ion velocity
distributions in the high-latitude ionosphere,
Rev. Geophys. Space Phys., 17, 99-134, 1979.

Suvanto, K., Ion cyclotron microinstability driven
by non-thermal F-region plasma, Planet. Space
Sci., in press, 1988a.

Suvanto, K., Microinstabilities driven by non-
thermal plasma in the high-latitude F-region,
Adv. Space Res., in press, 1988b.

Todd, H., B. J. I. Bromage, S. W. H. Cowley, M.
Lockwood, A. P. van Eyken, and D. W. Willis,
EISCAT observations of bursts of rapid flow in
the high-latitude dayside ionosphere, Geophys.
Res. Lett., 13, 909-912, 1986.

Tsunoda, R., R. C. Livingston, C. L. Rino, and J.
F. Vickrey, Dayside observations of thermal ion
upwelling at 800 km altitude: An ionospheric
signature of the cleft ion fountain, EOS,
Trans. AGU, 66(46), 1003, 1985.

Whalen, B. A., W. Bernstein, and P. W. Daly, Low
altitude acceleration of ionospheric ions,
Geophys. Res. Lett., 5, 55, 1978.

Winser, K. J., G. O. L. Jones, and P. J. S.
Williams, Variations in field-aligned plasma
velocity with altitude and latitude in the
auroral zone: EISCAT observations and physical
interpretation, Phys. Scr., 37, 640-644, 1987a.

Winser, K. J., M. Lockwood, and G. O. L. Jones,
Nonthermal plasma observations using EISCAT:
Aspect angle dependence, Geophys. Res. Lett.,
14, 957-960, 1987b.

Winser, K. J., G. O. L. Jones, P. J. S. Williams
and M. Lockwood, Observations of large field-
aligned flows of thermal plasma in the auroral
ionosphere, Adv. In Space Res., in press, 1988.

Yau, A. W. and M. Lockwood, Vertical ion flow in
the polar ionosphere, in "Modeling
Magnetospheric Plasma", Geophys. Monogr. Ser.,
44, AGU, Washington, D.C., 229-240, 1988.

Yau, A. W., B. A. Whalen, A. G. McMamera, P. G.
Kellog, and W. Bernstein, Particle and wave
observations of low altitude ionospheric ion
acceleration events, J. Geophys. Res., 88, 34,
1983.

Yau, A. W., E. G. Shelley, W. K. Peterson, and L.
Lenchyshyn, Energetic auroral and polar ion
outflow at DE 1 altitudes: Magnitude,
composition, magnetic activity dependence, and
long term variations, J. Geophys. Res., 90,
8417-8432, 1985.

T. J. Fuller-Rowell, University College, Gower
Street, London, WC1E 6BT England.
M. Lockwood, Rutherford Appleton Laboratory,
Chilton, Didcot, OX11 0QX England.
K. Suvanto, Blackett Laboratory, Imperial College,
London, SW7 2BZ, England.